ChemComm

Accepted Manuscript

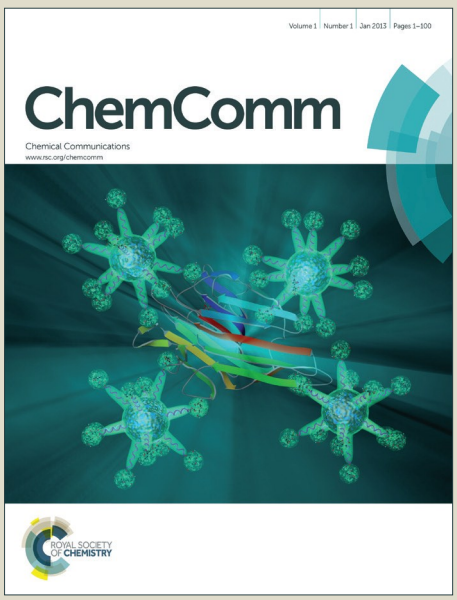

ROYAL SOCIETY OF CHEMISTRY

www.rsc.org/chemcomm

ChemComm

COMMUNICATION

Portable and Quantitative Monitoring of Mercury Ions Using DNA-gated Mesoporous Silica Nanoparticles with a Glucometer Readout

Received 00th January 20xx,
Accepted 00th January 20xx

DOI: 10.1039/x0xx00000x

www.rsc.org/

Xiaoling Liang, Lin Wang, Dou Wang, Lingwen Zeng* and Zhiyuan Fang*

A novel glucometer biosensor was developed for quantitative detection of mercury ions (Hg^{2+}) based on glucose loaded DNA-gated mesoporous silica nanoparticles (MSNs).

Hg^{2+} is a bioaccumulative and highly toxic pollutant that causes deleterious effects on human health even at low concentration.[1, 2] Inspired by the coordinative interaction between Hg^{2+} and bis-thymine that demonstrated by Ono and Togashi,[3] many fluorescent,[4] colorimetric[5] and electrochemical[6] sensors have been developed for Hg^{2+} detection in recent years. Compared with conventional methods (e.g. inductively coupled plasma mass spectroscopy, ICPMS), these novel assays are cost saving and have less requirements of instrumentations and skilled personnel. However, they still have limitations in the field of quantitative and portable detection of Hg^{2+}.

The personal glucose meter (PGM) is currently one of the most widely used diagnostic devices due to its portable size, easy operation, low cost and reliable quantitative results.[7, 8] Recently, Lu,[7, 9-11] and Yang[12] et al reported a series of methods by coupling functional DNA probes with a PGM for the detection of different analytes (e.g. metal ions, cocaine, virus and disease markers). However, these methods depended on hydrolytic enzymes, e.g. invertase or amylase, to produce glucose for glucometer readout, which made the multi-steps of washing/separation inevitable. New signal transduction strategies that provide simpler sample process while still allowing efficient conversion of target recognition events into a cascaded glucose production are thus highly desired.

MSNs with high colloidal stability are attracting growing attentions for their great potentiality in the field of nanomedicine.[13, 14] Molecular dynamic simulations revealed a strong and preferential interaction between glucose molecule and the silica wall, which trapped high concentration of glucose in the pore.[15] Recently, Fu[16] and Wang[17] have developed PGM-based assays using glucose loaded MSNs. In this regard, the aim of this work is to exploit a simple PGM-based assay for in field detection of Hg^{2+} using glucose loaded MSNs.

The detection of Hg^{2+} is based on the target-responsive release of glucose from single-strand wrapping DNA sealed MSNs (DNA-gated MSNs, Scheme 1). A noticeable amount of glucose molecules are firstly loaded into the pores of MSNs. After then, the gates of MSNs are sealed by single-stranded wrapping DNA based on the electrostatic attraction between positive charged aminated MSNs and negative charged DNA. Upon the addition of Hg^{2+} and assistant DNA, the T-Hg^{2+}-T base pairing can detach wrapping DNA from MSNs and induce the formation of wrapping and assistant DNA duplex. The formed duplex DNA is then recognized by Exo III, which can digest the wrapping DNA from 3'-hydroxyl terminus.[18] The digestion of wrapping DNA further releases Hg^{2+}, leading to the continuous detaching of wrapping DNA from MSNs. As a result, the "gate" is opened and allows the pore-trapped glucose diffuse out of MSNs for PGM readout. The signal intensity of PGM is proportional to the Hg^{2+} concentration.

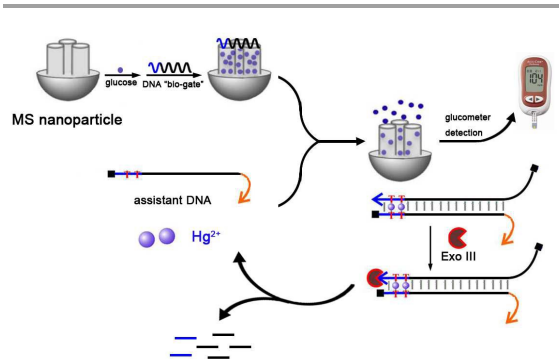

Scheme 1. Schematic illustration of DNA-gated MSNs based quantitative detection of Hg^{2+} with PGM readout.

Key Laboratory of Regenerative Biology, South China Institute for Stem Cell Biology and Regenerative Medicine, Guangzhou Institutes of Biomedicine and Health, Chinese Academy of Sciences, Key Laboratory of Guangdong province, Guangzhou 510530, China.
**Co-corresponding author. E-mail: zeng6@yahoo.com;fangjnu@126.com; Tel:+862032015312; Fax:+862032015245.*

Well prepared DNA-gated MSNs are crucial for the assay. Typical transmission electron microscopic (TEM, JEM-2100, JEOL Ltd., Japan) image of the as-prepared MSNs with an average diameter of 150 nm was shown in Figure 1A. The N_2 adsorption–desorption isotherm curve (ASAP 2000 Instrument, Micromeritics, Norcross, GA, USA) of the as-prepared MSNs presented a specific surface area of 1149.177 m^2/g (Fig. 1B). The MSNs also showed a narrow pore distribution and an average diameter of 2.7 nm based on Barrett–Joyner–Halenda (BJH) formula (inset of Fig. 1B). The diameter of pore was much larger than that of the glucose molecule (1.0 nm in diameter). Thus, a large number of glucose can be entrapped inside the MSNs. The new peaks at 2976 and 2933 cm^{-1} (circle part, Fig. 1C) showed in Fourier Transform Infrared Spectroscopy (FT-IR, Bruker Vertex 70 FT-IR Spectrometer) analyses corresponded to -CH^2- group of aminopropyl from 3-Aminopropyltriethoxysilane (APTES) molecules, which indicated the successful immobilization of APTES onto MSNs (Fig. 1C). Contributions from -NH^2- group were probably overlapped with vibration bands from silanol groups and adsorbed water. Furthermore, the sealing of "gate" by wrapping DNA was also confirmed by UV-vis absorption spectrometry (Techcomp, UV/vis 1102, China). An obvious characteristic DNA absorption peak at 265 nm was detected when wrapping DNA was assembled onto the surface of aminated MSNs (curve 'c', Fig. 1D). These results showed that the wrapping DNA was assembled onto the aminated MSNs successfully.

The loading efficiency of glucose was described in the supplementary information (Fig. S1, ESI†). The PGM signal in the presence of complementary oligonucleotide (c-DNA, 20 μM) and single mismatch assistant DNA (200 nM DNA, 10 nM Hg^{2+}) were 6.5 ±0.2 mM and 14.1±0.6 mM, respectively. The Hg^{2+} trigged glucose leakage from DNA-MSNs was comparable to that of c-DNA, which

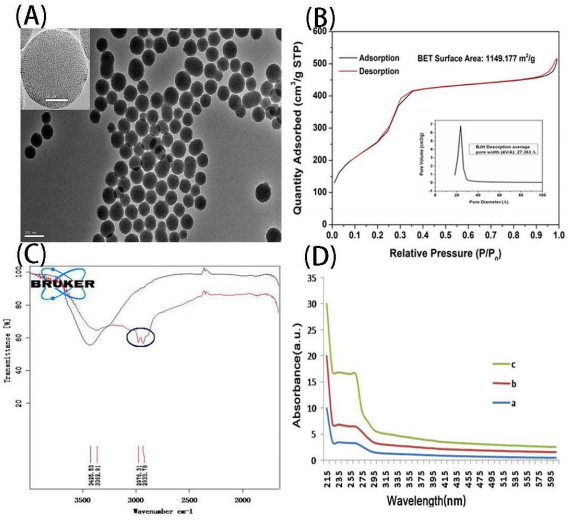

Fig. 1 (A) TEM image of the as-synthesized MSNs (inset: magnification image); (B) N_2 adsorption–desorption isotherms (inset: pore size distribution); (C) FTIR spectra of MSNs (black), APTES-functionalized MSNs (red); and (D) UV-vis absorption spectra of MSNs (a), APTES-functionalized MSNs (b) and DNA–MSNs (c).

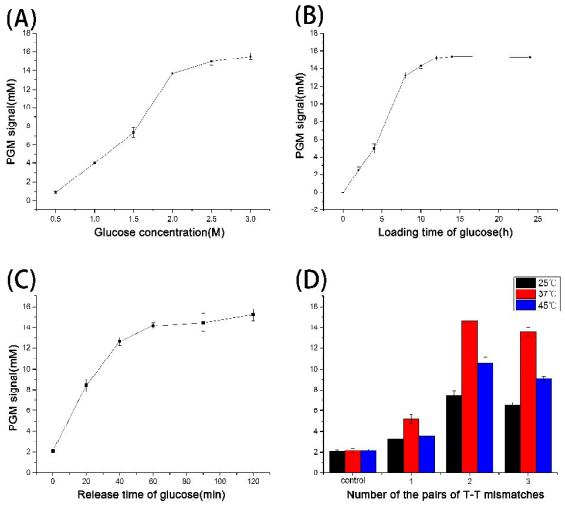

Fig. 2 Dependence of the PGM signal on (A) glucose concentration, (B) loading time of glucose, (C) release time of glucose and (D) number of the pairs of T-T mismatches and reaction temperature (10 nM Hg2+ used in this case).

indicated the successful capping and high efficient releasing capability of this method.

In the present assay, PGM signal mainly derives from entrapped glucose molecules in the pores of MSNs. Theoretically, the loading capacity depends directly on the concentration of glucose in the loading solution. As shown in Figure 2A, PGM signal increases with elevated concentration of glucose and reaches the balance beyond 2.0 M, which is used in the following studies. In addition, the loading amount of glucose also depends on the assembling time. Figure 2B presents the effect of the assembling time on PGM signal intensity (in 10 nM Hg^{2+}). The intensity of PGM signal increases with the increment of assembling time from 0 h to 10 h and tends to level off after 10 h. Hence, 10 h was used for the assembling of glucose. Figure 2C represents the time-dependent signal intensity changes upon Exo III digestion (i.e. the release time of glucose from the MSNs, excluding 20 min for the formation of T-Hg^{2+}-T base pair). The PGM signal increases with the elongation of detection time and reaches equilibrium after 40 min. To save the assay time, 40 min was used for the release of glucose in this assay. Furthermore, PGM signal was also affected by the number of T-T mismatches and reaction temperature (Fig. 2D). Effect of reaction temperature on PGM signal was firstly investigated using 10 nM Hg^{2+} at three different temperatures (25°C, 37°C, and 45°C). Blank control (in the absence of Hg^{2+}) was conducted at each temperature under the same conditions. Intensity of PGM signal increased as the reaction temperature elevated from 25°C to 37°C and then decreased from 37°C to 45°C (Fig. 2D). Therefore, 37°C was the optimum reaction temperature. Additionally, assistant DNA with two T-T mismatches showed higher PGM signal intensity than the others. Hence, the wrapping DNA and the assisted DNA with two T-T mismatches were used in the following experiments.

After optimization of parameters, the developed system was applied for quantifying Hg^{2+} standard solution. Reaction was carried out in 200 μL PCR tube containing 10 μL of DNA-MSNs suspension, 5

μL of Hg^{2+} standards (or samples) and 200 nM assistant DNA. After incubation at RT for 30 min, 20 units of Exo III were added to the above solution. The mixture was then incubated for another 30 min at room temperature on an end-over-end shaker. As illustrated in Figure 3A, the calibration plot displayed a good liner relationship between glucometer signal and Hg^{2+} concentration in the range from 0.1 nM to 80 nM. The linear regression equation was y = 7.14329x + 2.34724 (nM, R^2=0.9848, n=30). The detection limit (LOD) was 0.1 nM. As the maximum permissible contamination level of Hg^{2+} in drinking water defined by the United States Environmental Protection Agency (EPA) is 10 nM, this DNA-MSNs based biosensor holds great promise in on-site monitoring of Hg^{2+}.

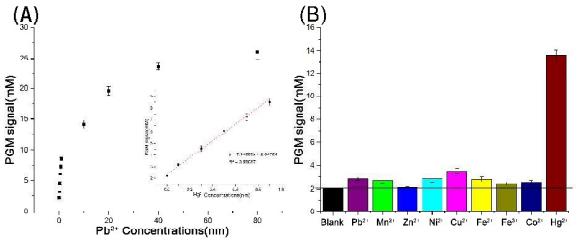

Fig. 3 (A) Calibration curve for PGM-based Hg^{2+} sensor using a range of standard Hg^{2+} concentrations. (B) The selectivity of the PGM-based Hg^{2+} sensor toward other metal ions (10 nM Hg^{2+} and 5.0 μM interfering ions used in this case). Each data point represents the average value obtained from three different measurements.

Selectivity of the DNA-MSN sensing system was evaluated by testing the response of this assay to other metal ions (5.0 μM), including Pb^{2+}, Mn^{2+}, Zn^{2+}, Ni^{2+}, Cu^{2+}, Fe^{2+}, Fe^{3+}, Cd^{2+}, and Co^{2+}. As illustrated in Figure 3B, the addition of 10 nM Hg^{2+} causes a significant increase in the PGM signal, showing obvious difference response from the other metal ions. Hence, the developed DNA-MSN-based assay could be used for specific detection of the target Hg^{2+} ions.

Reproducibility of this assay was investigated by testing 3 different Hg^{2+} standards. The results showed that coefficients of variation (CVs) of intra-assay (n=6,) were 4.2%, 3.3% and 3.6% for 40 nM, 10 nM and 1 nM of Hg^{2+}, respectively. The CVs of the inter-assay were 8.4%, 7.8% and 7.3%, respectively. The results showed good reproducibility of this assay.

To assess the performance of this assay in real sample analysis, several environmental water samples, including tap water and lake water, were tested. The samples spiked with different concentrations of Hg^{2+} were analyzed in triplicates. The results were summarized in Table S2 (ESI†). Satisfactory recovery rates between 96% and 108% were obtained, which shows that this assay is feasible for real environmental samples.

In summary, we demonstrated a simple and sensitive PGM-based assay for Hg^{2+} detection with large dynamic range and high sensitivity. Compare with standard instrumental sensing methods, the PGM-based assay has the advantage of being low-cost, rapid, portable and user-friendly, which can be more widely available for public use, particularly in developing countries.

This work was financially supported by Key Deployment Project of the Chinese Academy of Sciences (KSZD-EW-Z-021-1-4) and Strategic Cooperation Project of the Chinese Academy of Sciences and Guangdong Province (2012B091100267).

Notes and references

1. P. B. Tchounwou, W. K. Ayensu, N. Ninashvili and D. Sutton, *Environmental Toxicology*, 2003, **18**, 149-175.
2. E. M. Nolan and S. J. Lippard, *Chemical reviews*, 2008, **108**, 3443-3480.
3. A. Ono and H. Togashi, *Angewandte Chemie International Edition*, 2004, **43**, 4300-4302.
4. J. Du, M. Liu, X. Lou, T. Zhao, Z. Wang, Y. Xue, J. Zhao and Y. Xu, *Analytical chemistry*, 2012, **84**, 8060-8066.
5. D. Li, A. Wieckowska and I. Willner, *Angewandte Chemie*, 2008, **120**, 3991-3995.
6. D. Du, J. Wang, L. Wang, D. Lu and Y. Lin, *Analytical chemistry*, 2012, **84**, 1380-1385.
7. Y. Xiang and Y. Lu, *Journal*, 2011, **3**, 697-703.
8. K. Billingsley, M. K. Balaconis, J. M. Dubach, Z. Ning, E. Lim, K. P. Francis, H. A. Clark and A. Chem., *Analytical chemistry*, 2010, **82**, 3707-3713.
9. Y. Xiang and Y. Lu, *Chemical communications*, 2013, **49**, 585-587.
10. Y. Xiang and Y. Lu, *Analytical chemistry*, 2012, **84**, 4174-4178.
11. Y. Xiang and Y. Lu, *Analytical chemistry*, 2012, **84**, 1975-1980.
12. L. Yan, Z. Zhu, Y. Zou, Y. Huang, D. Liu, S. Jia, D. Xu, M. Wu, Y. Zhou, S. Zhou and C. J. Yang, *Journal of the American Chemical Society*, 2013, **135**, 3748-3751.
13. M. Colilla, B. González and M. Vallet-Regí, *Biomater. Sci.*, 2013, **1**, 114-134.
14. Q. He and J. Shi, *Advanced Materials*, 2014, **26**, 391-411.
15. A. Lerbret, G. Lelong, P. E. Mason, M.-L. Saboungi and J. W. Brady, *The Journal of Physical Chemistry B*, 2011, **115**, 910-918.
16. L. Fu, J. Zhuang, W. Lai, X. Que, M. Lu and D. Tang, *J.mater.chem.b*, 2013, **1**, 6123-6128.
17. Y. Wang, M. Lu, J. Zhu and S. Tian, *Journal of Materials Chemistry B*, 2014, **2**, 5847-5853.
18. R. Freeman, X. Liu and I. Willner, *Nano Letters*, 2011, **11**, 4456-4461.